This article is part of the

Proceedings of the 16th Minisymposium Verfahrenstechnik and 7th Partikelforum (TU Wien, Sept. 21/22, 2020)

Title:
Comparison of nasal breathing LB simulation results with rhinomanometry and acoustic rhinometry measurements

Corresponding author:
Manuel Berger (MCI - The Entrepreneurial School, Innsbruck - Dept. of Environmental, Process & Energy Engineering), manuel.berger@mci.edu

Date of submission:
10.02.20

Date of revision:
27.08.20

Date of acceptance:
27.08.20

Chapter ID:
DiV2-(02)

Length:
4 pages

Download available from (online, open-access):
http://www.chemical-engineering.at/minisymposium

ISBN (full book):
978-3-903337-01-5

Comparison of nasal breathing lattice Boltzmann simulation results with rhinomanometry and acoustic rhinometry measurements

Manuel Berger[1,2*], Martin Pillei[1,3], Andreas Mehrle[4], Wolfgang Recheis[5], Florian Kral[6], Wolfgang Freysinger[2] and Michael Kraxner[1]

1: Dept. of Environmental, Process & Energy Engineering, MCI Innsbruck, Austria, manuel.berger@mci.edu
2: Dept. of Oto- Rhino- Laryngology, Medical University Innsbruck, Austria
3: Dept. of Fluid Mechanics, Friedrich-Alexander-University Erlangen-Nürnberg, Germany
4: Dept. of Mechatronics, MCI Innsbruck, Austria
5: Dept. of Radiology, Medical University Innsbruck, Austria
6: Dep. of E.N.T., Kardinal Schwarzenberg Hospital, Schwarzach in Pongau, Austria

Keywords: rhinomanometry, acoustic rhinometry, lattice Boltzmann, nasal breathing, comparison

Abstract

The accuracy of simulation results to predict surgical outcome to improve nasal breathing is important to satisfy patients. Therefore, in the presented work lattice Boltzmann simulation results are compared to acoustic rhinometry and rhinomanometry data.

The basis is an already laser Doppler anemometry validated lattice Boltzmann code to simulate nasal breathing. To further investigate the quality of the simulation results, rhinomanometry and acoustic rhinometry data of a patient with nasal septum deviation are used for comparison. The lattice Boltzmann simulation is based on an air-segmented computer tomography dataset. Rhinomanometry and acoustic rhinometry are measurements to evaluate functionality of the nasal breathing process. Both methods are applied on the patient without and with a medication that the swelling of the mucosa is reduced.

Lattice Boltzmann simulations show that the results are closer to rhinomanometry without the medication that reduce the swelling of the mucosa. On the left side of the nasal cavity, the simulation is in comparison with rhinomanometry data, in between both measurements. In contrast to the right nasal cavity simulation predict a higher pressure drop (10 %) than rhinomanometry.
Segmentation compared to acoustic rhinometry shows up to a distance of 6 cm from the nostril good accordance. However, surgeons experience is that acoustic rhinometry is at bigger distances not trustful anymore.

Based on the presented result there is the conclusion that the segmentation process of the CT dataset is a good way to get a digital twin of the nasal cavity that can be used for numerical simulations. As expected simulation and measurements are not coincident. Based on the presented results there is no need to change the segmentation process or imaging technique.

Introduction

Since studies show that 30.9 % of patients in ENT [1] departments of hospitals have a nasal septum deviation and the success rate is only between 65 % and 80 % [2], there is the need to support surgeons with novel approaches. Support is performed either during the surgery (intraoperative) or in the preoperative planning.
In the preoperative planning, simulation techniques to simulate the flow through the nasal cavity could help finding regions with high pressure drop that indicate a constriction as presented at the Minisymposium Process Engineering 2019 in Leoben [3]. The used lattice Boltzmann (LB) simulation based on Sailfish CFD [4] is validated already by laser Doppler anemometry (LDA) measurements [5]. Patient data based on rhinomanometry and acoustic rhinometry allow a further comparison.
So far, the quality of the segmentation process is not taken into account since LDA and LB are based on the same dataset. There is no proof whether the segmentation process based on CT image of the nasal cavity accurate enough. However, there is one publication that shows that thresholding with -460 Hounsfield units [6] to perform air segmentation in the computer tomography (CT) dataset is a good choice. The CT dataset is limited to image air and the nasal mucosa [7] that might influence the quality of the simulation result. Therefore, of a patient with nasal septum deviation a CT dataset, rhinomanometry and acoustic rhinometry measurement are used for the investigation.
CT allows to give a three-dimensional inside into the human body by x-rays [8] that is so far the state-of-the-art available imaging technique with the disadvantage of radiation exposure.
Rhinomanometry controls the air flow rate through the nasal cavity of left and right side separately and measure the pressure drop between nostril and throat [9]. It generates a “system curve” of the nasal cavity to differentiate between a geometrical problem or a swelling of the nasal mucosa. Acoustic rhinometry determines the air flow cross-section as a function of the distance from the nostril by acoustic waves [9] of left and right channel of the nasal cavity separately to find the constrictions that causes the breathing problem.
The fluid flow simulation method LB is chosen since it is easy to apply and numerically stable on complex geometries. Sailfish CFD features GPU (graphical processing unit) support and fast computation (less than 5 minutes) to know the velocity vector field and pressure scalar field of the nasal breathing process.
The topics investigated in this study are to find the accuracy of the LB simulation with segmentation process by a comparison with rhinomanometry and acoustic rhinometry data. Therefore, in the segmentation process for the simulation the left or right nasal cavity is locked. The outcome should be a decision whether there is the need for changes in the CT segmentation process, or whether there is the need for a different imaging method like magnetic resonance imaging (MRI).

Methods

Segmentation of the CT dataset

An anonymous patient CT dataset with a nasal septum deviation and a resolution of 0.3 x 0.3 x 0.3 mm³ from Siemens Somatom is air segmented by thresholding to -460 Hounsfield units [6]. To define a label map of the voxels inside the nasal cavity, at the nostril and throat a horizontal cut is defined. Subsequently, a region growing algorithm removes the voxels outside the nasal cavity. By a marching cubes algorithm [10], a surface geometry file is generated and saved in stl format. In Blender [11] at the nostril and throat a cuboid is added to define mass flow rate by a velocity boundary condition later on at the fluid flow simulations. Since at rhinomanometry investigation the left or right side of the nasal cavity is investigated separately, at the stl surface geometry one nostril is locked, created by a Boolean operation, as depicted in Fig. 1. All segmentation operations are performed in 3D Slicer [12], an open source software for medical image informatics, image processing, and three-dimensional visualization. Fig. 1 shows the triangles of the stl surface geometry with the locked nostril.

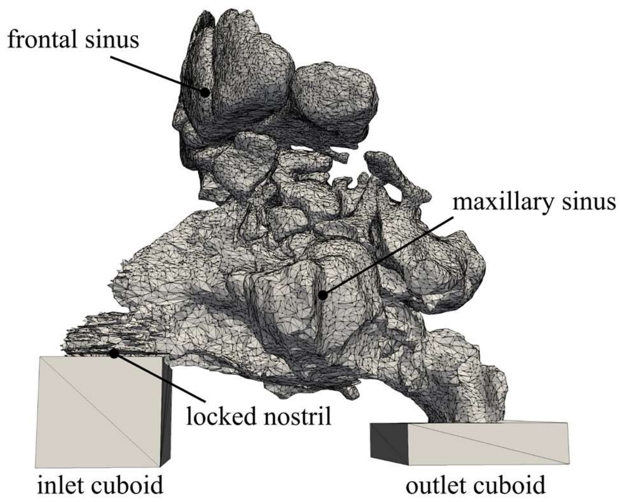

Fig. 1: Air segmented nasal cavity saved in stl format. The cuboids at the inlets and outlets are used for setting the boundary conditions at the fluid flow simulation. In total there are two stls, one is locked at the left nostril, the other one at the right nostril.

Lattice Boltzmann simulations of the nasal cavity

For the lattice Boltzmann (LB) fluid flow simulations the python based framework Sailfish CFD [4] with GPU implementation is used. In order to deal with turbulent structures at a flow rate higher than 300 ml/s the LES turbulence model Smagorinsky Lilly with cs = 0.14 [4] is used. The turbulence model is used since temporal and spatial resolution is computationally limited to resolve turbulent structures. With artificial viscosity in average turbulent structures are modelled. This critical flow rate was determined by Reynolds number calculation compared to a critical Reynolds number in a pipe with 2300 [13]. The flow boundary condition is taken from rhinomanometry. Since the result is a continuous pressure/flow rate curve, there would be the need for infinite amount of simulations. To recalculate the curve a discretization of 50 ml/s is chosen. With a maximum flow rate boundary from rhinomanometry (600 ml/s), there are 12 simulations for inhalation/exhalation of left and right side of the nasal cavity (48 simulations). The simulations were initialized with $\vec{v} = 0$ and stopped when the pressure drop between inlet and outlet converged, after 0.025 seconds simulation time. The overall computational time of one simulation is smaller than 5 minutes. The spatial resolution of the LB simulation was chosen based on experience of previous investigations [14] so that the result is mesh independent. This pressure drop between nostril and throat is taken for comparison with the rhinomanometry.

Cross-section determination for comparison with acoustic rhinomanometry

For the comparison of segmentation with acoustic rhinometry, the coronal air flow cross-section must be determined in the CT dataset. The basis is the surface geometry file in stl generated by the segmentation process in 3D Slicer. Coronal cross-sections with a spatial discretization of 5 mm are chosen (coronal distance from the nostril). In total 19 cross-sections are investigated. The cross-section calculation is performed by numerical integration of the surface integral

$$\iint \mathrm{dxdy},$$

where x and y are the spatial coordinates in the coronal investigation plane. The numerical calculation is performed in ParaView [15]. So this investigation is independent of the simulation, this is just a comparison of the segmentation process with cross-section determined by acoustic rhinometry.

Results

Fig. 2 depicts the comparison between LB simulation results of the segmented nasal cavity based on the CT dataset and rhinomanometry data of the same patient. Results colored in red show flow through the left nostril, whereas the right nostril was locked. Results colored in blue investigated the flow through the left nostril, whereas the right nostril was locked. Points with a black stroke are LB simulated data, all the other depicted data are the results of rhinomanometry digitized by WebPlotDigitizer [16].

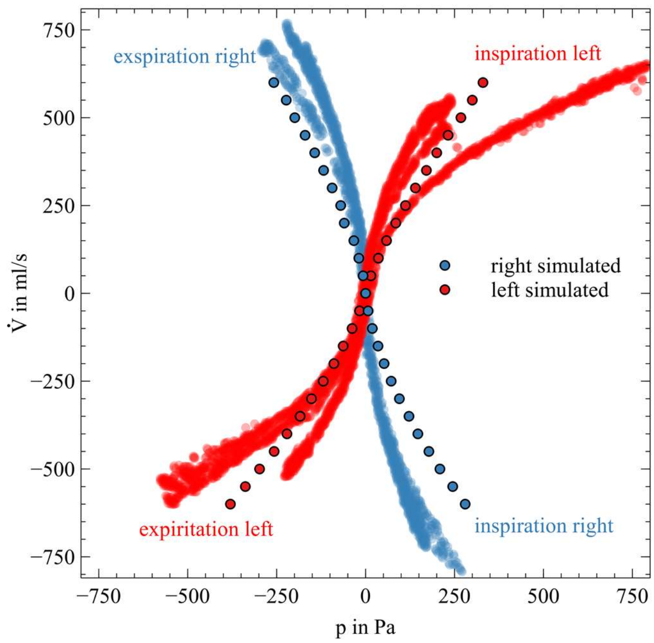

Fig. 2: Comparison of simulated data with rhinomanometry data. In the measurement are basically two curves, one originates from the initial, the second one with a

decongestant of the mucosa, where there is a pressure drop decrease.

The rhinomanometry measurement consists of two investigations: An initial one with higher pressure drop, and a second one where with a medication the swelling of the mucosa is reduced, with a lower pressure drop. So on locations where there is a big difference in both rhinomanometry measurements, it is not a geometrical breathing problem like a nasal septum deviation, but a swelling problem of the mucosa. At the simulations of the left side of the nasal cavity, the simulated results are in between both rhinomanometry curves. Thus, thresholding, the main important step in the segmentation process, represents the shape well. At the inspiration curves the simulated pressure drop is higher than the measured one by rhinomanometry.

Fig. 3 shows a comparison between acoustic rhinometry data and the coronal cross-section calculations of the segmentation process performed in ParaView. Again, the curve with less cross-section is due to swelling of the mucosa. The distance in cm is measured in coronal direction from the nasal tip. The reason for negative distance at the acoustic rhinometry data is because the sensor is put on the nostril and outside. On the acoustic rhinometry data one can see that the mucosa is present after 2.5 cm distance from the nostril. In general, the cross-section determination on the based on the CT dataset is closer to the smaller cross-section with a swelling of the mucosa. Medical doctors experience is that acoustic rhinometry data is trustful only the first 5 cm of the nostril.

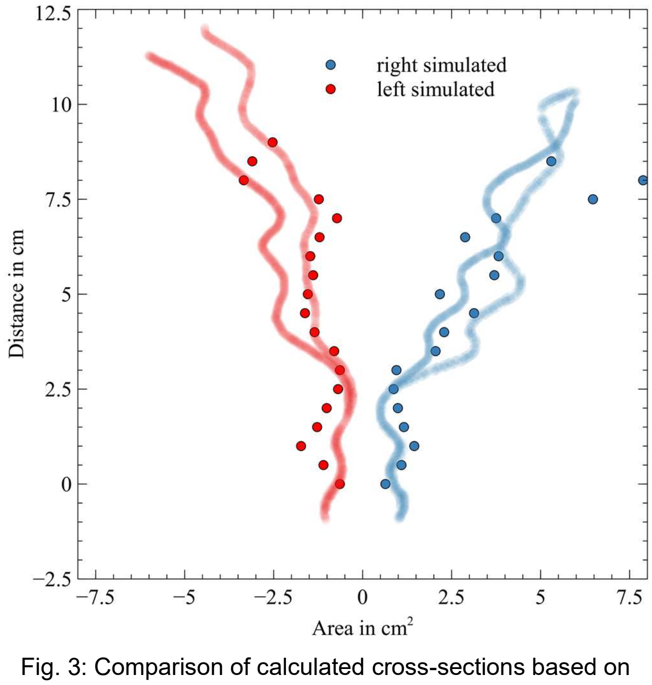

Fig. 3: Comparison of calculated cross-sections based on segmentations with acoustic rhinometry data. In the measurement there are basically two curves, one originates from the initial, the second one with a decongestant of the mucosa, where there is a cross-section increase.

Conclusion

Simulations are just as good as the underlying model and geometry is. In previous investigations, a lot of numerical simulations to support surgeons in the preoperative planning were performed. Some of them are not validated by experimental investigations [17]–[26]. Contrary, validation is performed in [27]–[32].

None of them have proofed, whether the segmentation process and the imaging technique is sufficient. Therefore, in this study rhinomanometry and acoustic rhinometry data are compared with patient CT data and the corresponding lattice Boltzmann simulation. From the results one can see that there are differences between imaging and measurements of the nasal cavity and the paranasal sinus. This is because the anatomy consists of different densities, i.e. bone, air, mucosa and not all can be imaged with CT in a good way.

At least one publication [6] tried to find the best thresholding value for air in a CT image to extract the nasal cavity. Since we used the same value, we see that this is not a bad assumption.

The next step is to repeat this study with more CT, rhinomanometry and acoustic rhinometry dataset to further proof the results presented in this paper.

Literature

[1] V. Sriprakash, “Prevalence and clinical features of nasal septum deviation: a study in an urban centre,” *Int. J. Otorhinolaryngol. Head Neck Surg.*, vol. 3, no. 4, p. 842, 2017, doi: 10.18203/issn.2454-5929.ijohns20173670.

[2] G. S. Gillman, A. M. Egloff, and C. M. Rivera-Serrano, “Revision septoplasty: A prospective disease-specific outcome study,” *Laryngoscope*, vol. 124, no. 6, pp. 1290–1295, 2014, doi: 10.1002/lary.24356.

[3] M. Berger *et al.*, “Methods to find surgically relevant points at breathing problems in the nasal cavity,” *Minisymp. Verfahrenstechnik*, 2019.

[4] M. Januszewski and M. Kostur, “Sailfish: A flexible multi-GPU implementation of the lattice Boltzmann method,” *Comput. Phys. Commun.*, vol. 185, no. 9, pp. 2350–2368, 2014, doi: 10.1016/j.cpc.2014.04.018.

[5] M. Berger *et al.*, “Flow measurement investigations of CFD based prediction tools for airflow in paranasal sinus,” *GALA-German Assoc. Laser Anemomentry*, no. 24, 2016.

[6] H. Nakano *et al.*, “A new method for determining the optimal CT threshold for extracting the upper airway,” *Dentomaxillofacial Radiol.*, vol. 42, no. 3, pp. 1–3, 2013, doi: 10.1259/dmfr/26397438.

[7] M. Nazri, S. I. Bux, T. F. Tengku-Kamalden, K.-H. Ng, and Z. Sun, “Incidental detection of sinus mucosal abnormalities on CT and MRI imaging of the head.,” *Quant. Imaging Med. Surg.*, vol. 3, no. 2, pp. 82–88, 2013, doi: https://dx.doi.org/10.3978/j.issn.2223-4292.2013.03.06.

[8] G. Zeng, *Medical Image Reconstruction: A Conceptual Tutorial*. Springer Berlin Heidelberg, 2010.

[9] R. Probst, G. Grevers, and H. Iro, *Basic otorhinolaryngology: a step-by-step learning guide*. Thieme, 2005.

[10] W. E. Lorensen and H. E. Cline, “Marching cubes: A high resolution 3D surface construction algorithm,” *Proc. 14th Annu. Conf. Comput. Graph. Interact. Tech. - SIGGRAPH ’87*, vol. 21, no. 4, pp. 163–169, 1987, doi: 10.1145/37401.37422.

[11] “Blender - a 3D modelling and rendering package,” *Blender Online Community*, vol. Blender Fo, no. Blender Institute, Amsterdam.

[12] et al Fedorov, A, “3D Slicer as an Image Computing Platform for the Quantitative Imaging Network,”

Magn. Reson. Imaging, vol. Nov;30(9), p. 18, 2012.

[13] L. D. Landau and J. M. Lifshitz, *Fluid Mechanics - Third Revised English Edition*. Pergamon, 1959.

[14] M. Berger *et al.*, “A mesh convergence study on LB flow simulations of the nasal geometry with horizontal cut,” *Minisymp. Verfahrenstechnik*, 2017.

[15] J. Ahrens, B. Geveci, and C. Law, “ParaView: An End-User Tool for Large Data Visualization,” *Elsevier*, 2005.

[16] A. Rohatgi, “WebPlotDigitizer.” .

[17] S. Naftali, M. Rosenfeld, M. Wolf, and D. Elad, “The air-conditioning capacity of the human nose,” *Ann. Biomed. Eng.*, vol. 33, no. 4, pp. 545–553, 2005, doi: 10.1007/s10439-005-2513-4.

[18] X. B. Chen, S. C. Leong, H. P. Lee, V. F. H. Chong, and D. Y. Wang, “Aerodynamic effects of inferior turbinate surgery on nasal airflow - A computational fluid dynamics model,” *Rhinology*, vol. 48, no. 4, pp. 394–400, 2010, doi: 10.4193/Rhino09.196.

[19] S. Ishikawa, T. Nakayama, M. Watanabe, and T. Matsuzawa, “Visualization of Flow Resistance in Physiological Nasal Respiration,” *Arch. Otolaryngol. Neck Surg.*, vol. 132, no. 11, p. 1203, 2006, doi: 10.1001/archotol.132.11.1203.

[20] X. B. Chen, H. P. Lee, V. F. H. Chong, and D. Y. Wang, “Numerical simulation of the effects of inferior turbinate surgery on nasal airway heating capacity,” *Am. J. Rhinol. Allergy*, vol. 24, no. 5, pp. 118–122, 2010, doi: 10.2500/ajra.2010.24.3511.

[21] S. Ozlugedik *et al.*, “Numerical Study of the Aerodynamic Effects of Septoplasty and Partial Lateral Turbinectomy,” *Laryngoscope*, vol. 118, no. 2, pp. 330–334, 2008, doi: 10.1097/MLG.0b013e318159aa26.

[22] S. Naftali, R. C. Schroter, R. J. Shiner, and D. Elad, “Transport phenomena in the human nasal cavity: a computational model.,” *Ann. Biomed. Eng.*, vol. 26, pp. 831–9, 1998, doi: 10.1114/1.108.

[23] Y. De Wang, H. P. Lee, and B. R. Gordon, “Impacts of fluid dynamics simulation in study of nasal airflow physiology and pathophysiology in realistic human three-dimensional nose models,” *Clin. Exp. Otorhinolaryngol.*, vol. 5, no. 4, pp. 181–187, 2012, doi: 10.3342/ceo.2012.5.4.181.

[24] D. Wexler, R. Segal, and J. Kimbell, “Aerodynamic Effects of Inferior Turbinate Reduction,” *Arch. Otolaryngol. Neck Surg.*, vol. 131, no. 12, p. 1102, 2005, doi: 10.1001/archotol.131.12.1102.

[25] G. J. M. Garcia *et al.*, “Atrophic rhinitis : a CFD study of air conditioning in the nasal cavity,” *PLoS One*, vol. 27709, pp. 1082–1092, 2007, doi: 10.1152/japplphysiol.01118.2006.

[26] H. P. Lee, H. J. Poh, F. H. Chong, and D. Y. Wang, “Changes of airflow pattern in inferior turbinate hypertrophy: A computational fluid dynamics model,” *Am. J. Rhinol. Allergy*, vol. 23, no. 2, pp. 153–158, 2009, doi: 10.2500/ajra.2009.23.3287.

[27] I. Hörschler, M. Meinke, and W. Schröder, “Numerical simulation of the flow field in a model of the nasal cavity,” *Comput. Fluids*, vol. 32, no. 1, pp. 39–45, 2003, doi: 10.1016/S0045-7930(01)00097-4.

[28] I. Weinhold and G. Mlynski, “Numerical simulation of airflow in the human nose,” *Eur. Arch. Oto-Rhino-Laryngology*, vol. 261, no. 8, pp. 452–455, 2004, doi: 10.1007/s00405-003-0675-y.

[29] D. J. Doorly, D. J. Taylor, and R. C. Schroter, “Mechanics of airflow in the human nasal airways,” *Respir. Physiol. Neurobiol.*, vol. 163, no. 1–3, pp. 100–110, 2008, doi: 10.1016/j.resp.2008.07.027.

[30] D. . Doorly, D. . Taylor, A. . Gambaruto, R. . Schroter, and N. Tolley, “Nasal architecture: form and flow,” *Philos. Trans. R. Soc. A Math. Phys. Eng. Sci.*, vol. 366, no. 1879, pp. 3225–3246, 2008, doi: 10.1098/rsta.2008.0083.

[31] Y. Na, K. S. Chung, S. K. Chung, and S. K. Kim, “Effects of single-sided inferior turbinectomy on nasal function and airflow characteristics,” *Respir. Physiol. Neurobiol.*, vol. 180, no. 2–3, pp. 289–297, 2012, doi: 10.1016/j.resp.2011.12.005.

[32] G. E. Heo, A. Seo, R. E. Kim, S. W. Kim, and S. K. Kim, “Experimental and numerical investigations on the flow field inside pre- and post-surgery models of posterosuperior septectomy,” *10th Int. Symp. Part. Image Velocim. - PIV13*, pp. 3–8, 2013.